

# Rethinking the 67 Hz QPO in GRS 1915+105: type-C QPOs at the innermost stable circular orbit

S.E. Motta<sup>1</sup> and T.M. Belloni<sup>1,\*</sup>

<sup>1</sup>Istituto Nazionale di Astrofisica, Osservatorio Astronomico di Brera, via E. Bianchi 46, 23807 Merate (LC), Italy  
e-mail: sara.motta@inaf.it

Received July 1, 2023; accepted January 30, 2024

## ABSTRACT

**Context.** The study of Quasi-Periodic Oscillations (QPO) at low and high frequency in the variability of the high-energy emission from black-hole binaries and their physical interpretation in terms of signatures of General Relativity in the strong-field regime.

**Aims.** To understand the nature of the 67 Hz QPOs observed in the X-ray emission of the peculiar black-hole binary GRS 1915+105 within the general classification of QPOs, and to determine the spin of the black hole in the system by applying the Relativistic Precession Model (RPM).

**Methods.** Within the RPM, the only relativistic frequency that is stable in time over a large range of accretion rates and can be as low as 67 Hz (for a black-hole mass as measured dynamically) is the nodal frequency at the Innermost Stable Circular Orbit (ISCO). In the application of the model, this corresponds to type-C QPOs. Under this assumption, it is possible to measure the spin of the black hole by using the mass of the black hole previously obtained via dynamical measurements. We re-analysed a large number of RossiXTE observations to check whether other timing features confirm this hypothesis.

**Results.** The identification of the 67 Hz QPO as the nodal frequency at ISCO yields a value of  $0.706 \pm 0.034$  for the black hole spin. With this spin, the only two QPO detections at higher frequencies available in the literature are consistent with being orbital frequencies at a radius outside ISCO. The high-frequency bumps often observed at frequencies between 10 and 200 Hz follow the correlation expected for orbital and periastron-precession frequencies at even larger radii.

**Key words.** X-ray: binaries – accretion, accretion disks – relativistic processes – black hole physics – stars: black holes

## 1. Introduction

Quasi-periodic oscillations (QPOs) are variability features frequently observed in the X-ray emissions of compact objects undergoing accretion. These oscillations are believed to originate from the innermost regions of the accretion flow. In a power density spectrum (PDS), QPOs manifest as relatively narrow peaks and their centroid frequency can be linked to dynamic motion and/or accretion-related time scales. QPOs have been known for several decades, yet their precise nature remains enigmatic. Numerous models have been proposed to explain their origin, leading to ongoing debates in the field (see Ingram & Motta 2019, for a recent review).

At low frequencies (< 30 Hz), three “flavors” of QPO have been observed in black-hole (BH) X-ray binaries (e.g., Wijnands & van der Klis 1999; Remillard et al. 2002; Casella et al. 2004, 2005). The most common of these types of QPO - called Type-C QPOs (Casella et al. 2005) - has a centroid frequency that can vary over a broad range (~0.1-30Hz). Although other models have been proposed (see, e.g. Belloni & Stella 2014, for a review), type-C QPOs have been often explained as a manifestation of the nodal (or Lense-Thirring<sup>1</sup>) precession of plasma orbiting around the BH (e.g., Stella & Vietri 1998; Ingram et al. 2009). They have also been associated to QPOs observed in neutron-star (NS) X-ray binaries, called Horizontal Branch Oscillations (HBO), suggesting that the same process is at work in both classes of systems

(Psaltis et al. 1999; Casella et al. 2005; Motta et al. 2017). In addition, QPOs with centroid frequencies above hundred Hz (up to ~500 Hz), although very rarely, have been observed from a small number of BH systems (e.g., Belloni et al. 2012), either isolated or, in an even smaller number of cases, in pairs. Such high-frequency oscillations are referred to as high-frequency QPOs (HFQPOs).

Within the Theory of General Relativity (GR), a particle in a bound orbit around a massive object, together with the orbital frequency ( $\nu_\phi$ ), has two additional frequencies associated to it, the vertical and radial epicyclic frequencies ( $\nu_\theta$  and  $\nu_r$ , respectively). From these frequencies, one can easily calculate two additional frequencies associated to the orbit: the nodal precession frequency ( $\nu_{\text{nod}} = \nu_\phi - \nu_\theta$ ), and the periastron precession frequency ( $\nu_{\text{per}} = \nu_\phi - \nu_r$ ). The gas accreting onto a BH can be seen as made of orbiting particles and therefore it is possible that the observed characteristic time scales yielded by the QPOs are the products of relativistic effects which can be associated to the aforementioned frequencies. If this association is established, it represents a powerful diagnostic tool for both GR in the strong-field regime, and the physics of accretion.

Along these lines, the Relativistic Precession Model (RPM) Stella & Vietri 1998; Stella et al. 1999; Stella & Vietri 1999) associates the nodal, periastron precession, and orbital frequency with the type-C QPO and the two HFQPOs - lower and upper, respectively - observed in the light curves of accreting BHs and NSs. For BHs, the number of detections of HFQPOs is very low and they are visible together with a type-C QPO even more rarely. Despite the scarcity of data, Motta et al. (2014a,b, 2022) showed that the RPM can be associated to the QPOs and broad noise

\* Deceased.

<sup>1</sup> The Lense-Thirring precession frequency is a weak-field approximation of the nodal precession frequency, see Stella & Vietri (1998).

components observed in the the BH binaries GRO J1655-40, XTE J1550-564 and XTE J1859+226. These works showed that the application of the RPM allows the self-consistent estimate of both spin and mass of a BH from timing features.

The bright BH binary GRS 1915+105 went into outburst in 1992 and is still active, although in a low-flux state (see, e.g., Motta et al. 2021). This system is known to be rather peculiar, displaying extreme structured variability on time scales above the second (see Fender & Belloni 2004, for a review). Despite these peculiarities, the PDS from GRS 1915+105 is not unlike that of other BH binaries, and strong type-C QPOs have been observed in its harder states (e.g., Markwardt et al. 1997; Ratti et al. 2012). At high frequencies, at variance with other systems, GRS 1915+105 has shown a number of features which have been classified as HFQPOs. In particular, a peak around 67 Hz has been consistently detected with RossiXTE for the sixteen years of operation of the satellite and in the past few years also by *Astrosat* (see, e.g., Morgan et al. 1997; Belloni & Altamirano 2013b; Belloni et al. 2019). This QPO was never observed together with a type-C QPO and represents a very stable frequency in the system.

In this paper we show that the features that until now have been classified as HFQPOs in GRS 1915+105 are instead consistent with being type-C QPOs produced near the innermost stable circular orbit (ISCO). Based on this assumption, we infer the spin of the BH hosted in GRS 1915+105, and we show that the inferred spin, coupled with the dynamical BH mass measurement, can be used to predict theoretical frequencies that match the data.

## 2. Rethinking the 67 Hz QPO

Belloni & Altamirano (2013b) reported a compilation of all the HFQPOs found in a systematic search performed on all the available RXTE data on GRS 1915+105. The centroid frequencies of 49 of the 51 peaks reported in such a work are found between 58 and 72 Hz (a histogram of such frequencies is shown in Fig. A.1). The two remaining peaks, detected at  $\sim 134$  and 143 Hz, are discussed in Sec. 3.1.

The frequencies of such 49 QPOs are distributed in a narrow range centred around 67 Hz, and henceforth we will refer to these QPOs collectively as *the 67 Hz QPOs*, aware that in reality they span a range of frequencies. Such a narrow range implies that they are determined by a parameter that - along with mass and spin - has to remain unchanged despite large swings in accretion rate. The most obvious candidate is the ISCO, which itself depends only on the mass and spin of the central black hole. The shape of the histogram in Fig. A.1 support the above fact, as it shows a clear drop at frequencies slightly above 67 Hz.

If we calculate the orbital frequency at ISCO (which at such a radius equals the periastron precession frequency) for a dimensionless spin parameter<sup>2</sup> (hereafter spin)  $a^* = 0$  and a mass of 14.4 (i.e. the upper limit on the mass based on the values reported by Reid et al. 2014,  $M = 12.4^{+2.0}_{-1.8} M_{\odot}$ ) we obtain  $\sim 152$  Hz<sup>3</sup>. This is the minimum possible orbital frequency in GRS 1915+105 at ISCO, as any larger BH spin value and any lower mass will yield higher frequencies. Thus, the 67 Hz QPOs are not consistent with being the result of the orbital motion of matter at the ISCO.

An intriguing possibility is that the 67 Hz QPO is the result of nodal precession at the ISCO. This would imply that the oscil-

lations observed around 67 Hz are *not* HFQPOs, as it has been believed for decades, but are instead type-C QPOs arising from very close to the ISCO. In this scenario, 67 Hz is the maximum possible centroid frequency for a type-C QPO for a given BH mass and spin. Consequently, the 67 Hz QPOs in GRS 1915+105 represent the high-frequency end of a broad distribution that includes all type-C QPOs in this system, which are most commonly observed below 10 Hz. The fact that a 67 Hz QPO has never been concurrently observed with another type-C QPO supports this hypothesis. This perspective also coherently clarifies why GRS 1915+105, unlike other BH X-ray binaries, exhibits numerous PDS peaks identified as HFQPOs: the 67 Hz QPOs would be reclassified not as HFQPOs, which are relatively rare in BH X-ray binaries, but rather as type-C QPOs, a more frequent occurrence in these systems.

To the best of our knowledge, current literature lacks efforts to interpret the  $\sim 67$  Hz QPOs in GRS 1915+105 as anything other than HFQPOs (Morgan et al. 1997). Alternative models have been previously proposed (see, e.g., Fragile et al. 2016; Ingram & Motta 2019) that could offer different interpretations of these QPOs, and which could be tested using the data considered here (all available in the literature). However, conducting such tests falls outside the scope of of this work.

In the scenario we have outlined, three facts are worth mentioning. Firstly, the 67 Hz QPOs do not exhibit characteristics typical of Type-C QPOs. Secondly, there are additional QPOs identified in GRS 1915+105 with frequencies close yet inconsistent with the 67 Hz QPOs (Belloni & Altamirano 2013a, and references therein). Finally, at least one other source has been observed to exhibit a QPO at approximately 67 Hz. We discuss each of these points in detail below.

At first glance the 67 Hz QPOs do not show the typical characteristics of type-C QPOs. While type-C QPOs at lower frequencies are generally superimposed on broad-band variability, the 67 Hz QPOs distinctively emerge from the Poisson noise. Additionally, these QPOs exhibit a relatively low rms amplitude (lower than 1%). These properties should not surprise. Firstly, the broad band variability typical of BH XRBs which always shows a cut-off between a few tenths of Hz and at a few Hz). Consequently, as the frequency of a QPO increases, it becomes increasingly probable for it to arise from Poisson noise rather than from broad-band variability. A similar situation can be observed in GRO J1655-40, where Type-C QPOs observed in the soft state are observed at around 30 Hz in a region of the PDS which is Poisson-noise dominated. Furthermore, the amplitude of type-C QPOs is anti-correlated with the centroid frequency, and thus higher frequency oscillations are expected to show lower amplitudes (see, e.g., Motta et al. 2015).

Several authors reported the discovery of various QPO peaks in the PDS from GRS 1915+105, at 27 (Belloni et al. 2001), 34 (Belloni & Altamirano 2013a) and 41 Hz (Strohmayer 2001). The 34 Hz QPO can be readily interpreted as harmonically related to the 68 Hz QPO observed in the same PDS. This harmonic relationship is a common feature of Type-C QPOs, which makes the above unsurprising. Even the occurrence of an isolated 34 Hz QPO (i.e., without a concurrent higher frequency harmonic peak) would not be unexpected. This is due to the variable amplitude of harmonically-related peaks observed in several X-ray binaries, particularly in neutron star systems, where the most prominent, and sometimes the only significant QPO peak does not necessarily correspond to the fundamental frequency of the modulation underlying the signal (Motta et al. 2017). Consequently, the detection of an *orphan* 27 Hz peak might be interpreted in a similar way, pre-

<sup>2</sup> The dimensionless spin parameter is defined as  $a^* = J/M^2$ , where  $J$  is the BH angular momentum and  $M$  its mass.

<sup>3</sup> Note that we deliberately ignore solutions where the spin is counter rotating, based on the assumption that the BH spin and the angular momentum of the matter in the accretion disk are unlikely to be anti-parallel (Motta et al. 2018, for a discussion).

suming an undetected fundamental peak at approximately 54 Hz. It is more challenging to provide a straightforward explanation for the 41 Hz frequency reported in Strohmayer (2001), which was detected concurrently with the 67 Hz QPO, and yet appears to be unrelated to it. We hypothesise that these two QPOs, despite being observed in the same dataset spanning over 15 ks, might not be occurring strictly simultaneously. Under this assumption, the 41 Hz peak could be a type-C QPO at a lower frequency, with its frequency increasing to 67 Hz at a different time. However, this hypothesis requires further analysis for validation or refutation, a task we reserve for future work.

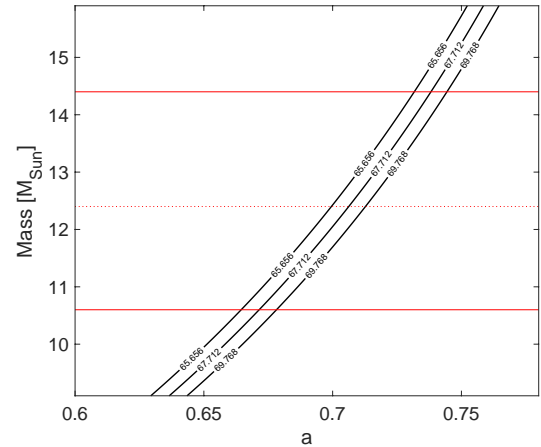
The 67 Hz QPO is not exclusive to GRS 1915+105 as a similar QPO at 66 Hz has been detected in the candidate BH X-ray binary IGR J17091-3624 during its first observed outburst (2011). Notably, this QPO was observed only once throughout all recorded outbursts of the source, although some excess in the PDS around 66 Hz and 164 Hz was detected in a number of observations of the same outburst (Altamirano et al. 2011). While we cannot exclude this possibility, current evidence does not support the conclusion that this QPO is of the same type as the 67 Hz QPO observed in GRS 1915+105. Nonetheless, it is intriguing that among known BH X-ray transients, the one exhibiting a QPO near 67 Hz shares phenomenological resemblances with those observed in GRS 1915+105 (Altamirano et al. 2011; Motta et al. 2021). This similarity warrants further investigation, particularly should any future data confirm that the 66 Hz modulation in IGR J17091-3624 shares properties with the 67 Hz QPOs in GRS 1915+105.

### 2.1. The spin

Under the intriguing hypothesis that the 67 Hz QPOs arise from nodal precession in the proximity of ISCO, it is possible to obtain an estimate of the BH spin as follows. First, we fit the histogram in Fig. A.1 with a Gaussian function, and we take the Gaussian's peak frequency as the frequency of the QPO arising at ISCO, and the Gaussian's FWHM as the 1-sigma error on such a frequency. This yield  $\nu_{nod@ISCO} = 67.7 \pm 2.1$  (see Tab. 1).

Next, we use the RPM to obtain an estimate of the spin. As described in Franchini et al. (2017), by substituting the expression of the radius of ISCO into the equation of the nodal precession frequency, one can remove the radial dependency and obtain an equations that only depend on the mass and spin of the BH. Adopting a BH mass of  $12.4^{+2.0}_{-1.8} M_{\odot}$  we obtain a spin of  $a^* = 0.706 \pm 0.034$ . The corresponding graphical solution is shown in Fig. 1. For this spin the radius of the innermost stable circular orbit radius is  $R_{ISCO} = (3.36 \pm 0.15) R_g$  (see Tab. 1).

As noted in Motta et al. (2022), we stress that if the RPM was an exact description of the behaviour of particles orbiting a BH, the uncertainties on the derived on the BH spin (and mass, and emission radius) would only come from the uncertainties on the measured QPO frequencies, which are dominated by the accuracy of the detecting instrument. However, the exact geometry of the emitting region is unknown, and so is the exact emission mechanism behind QPOs. Both the above facts (and likely others) might be sources of systematics. For instance, in Motta et al. (2022) we gauged the uncertainties that could be related with the the radial extent of the region originating the QPOs, and found that such systematics would be of the order 15%. Since the effective impact of systematics on the spin estimate is hard to determine accurately, we warn the reader that in the following - for simplicity and to avoid biases - we will report and use the uncertainties derived uniquely from the errors on the QPO centroid frequencies.



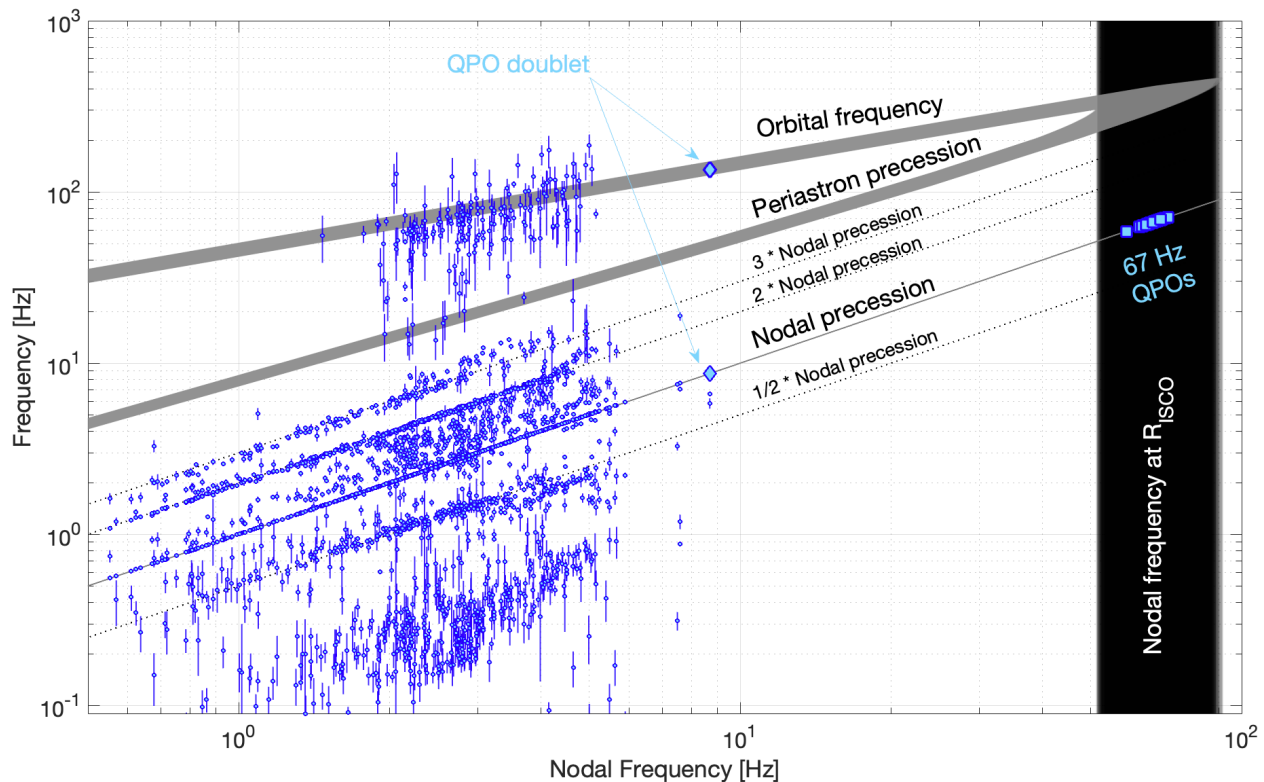


**Fig. 2.** Nodal precession frequencies (bottom grey line), periastron precession frequencies (middle lines), and orbital frequencies (top lines) plotted as a function of the nodal precession frequency, as predicted by the RPM using  $M = (12.4 \pm 0.46) M_{\odot}$  and  $a^* = 0.706 \pm 0.034$ . The set of lines forming grey regions in the figure each correspond to mass-spin pairs drawn from a bi-variate distribution (see main text). The lines corresponding to the Nodal precession Frequency overlap to each other as the Nodal precession frequency is the independent variable in this plot, hence the only difference between lines is in the maximum value they reach (i.e. the nodal precession frequency at ISCO). The dotted lines correspond to the sub-harmonic, the second and third harmonic of the nodal precession frequency. The vertical black lines correspond to the predicted nodal frequency at  $R_{\text{ISCO}}$  for the same pairs. For clarity we plot only the predicted frequencies for mass-spin pairs within  $1\text{-}\sigma$  from the central mass-spin value. The QPO doublet formed by a HFQPO at 135 Hz and a type-C QPO at 8.7 Hz are indicated by clear blue diamonds. The 67 Hz QPOs are marked by clear blue squares. All the PDS broad components described in Section 3.2 are marked by small blue dots with vertical error bars.

The inspection of the two PDS showing peaks at  $\sim 134$  and  $\sim 143$  Hz, respectively, reveals in both cases a clear LFQPO at  $\sim 6.5$  Hz. Such oscillations can be classified as a type-B QPO, based on their frequency and morphology (see, e.g., Casella et al. 2005; Motta et al. 2009). A close inspection of the PDS shows the presence of a weak peak at  $\sim 8.54$  Hz in one of the two cases, i.e. observation 50703-01-10-02, which according to Belloni & Altamirano (2013b) shows  $\rho$ -type variability). We classify the weak peak as a type-C QPO because it is not consistent with being the second harmonic to the modulation at 6.5 Hz, and because no type-B QPO has been observed above 7 Hz in GRS 1915+105 (see, e.g., Soleri et al. 2008). This PDS configuration, i.e. a type-B next to a weak type-C QPO, is relatively uncommon in BH X-ray binaries (Motta et al. 2015), but is typical of neutron star Z-sources (see, e.g., Motta & Fender 2019), which like GRS 1915+105 are believed to accrete near the Eddington limit (see Motta et al. 2017, for the case of Sco X-1)<sup>4</sup>.

We fitted the PDS as described in several works in the literature, with a number of Lorentzian shapes (e.g. Belloni et al. 2002). The best fit yields a type-C QPO frequency  $\nu_C = 8.71 \pm 0.09$  and a HFQPO at  $135.25 \pm 0.9$ . A plot showing the fitted PDS is shown in the appendix (Fig. A.2). Belloni & Altamirano (2013b) already showed that the HFQPO is formally significant after considering the number of trials. The type-C QPO, instead, is borderline significant, i.e. approximately  $3.1 \sigma$  single trial based on the QPO amplitude and its uncertainty. Determining the formal significance of a QPO super-imposed to a complex continuum (i.e., not simple red noise) is non trivial (see, e.g., Vaughan 2005), but for the sake of the argument, we will assume that the type-C QPO is correctly classified and statistically significant, and hence we will treat the tentative type-C QPO plus the HFQPO at  $\sim 143$  Hz as a QPO “doublet”. Marking this QPO “doublet” on the plot in Fig. 2 we see that the HFQPO peak is consistent with being a upper HFQPO, and can be associated with the orbital frequency according to the RPM. By extension and in virtue of their similar

<sup>4</sup> We note that the type-B and type-C QPOs that we detected are found at centroid frequencies in a  $4/3$  ratio. We believe that the fact that the two peaks are in a  $4/3$  ratio is pure coincidence as any slightly different

rebinning of the PDS results in slightly different centroid frequencies, which are not in a  $4/3$  ratio.

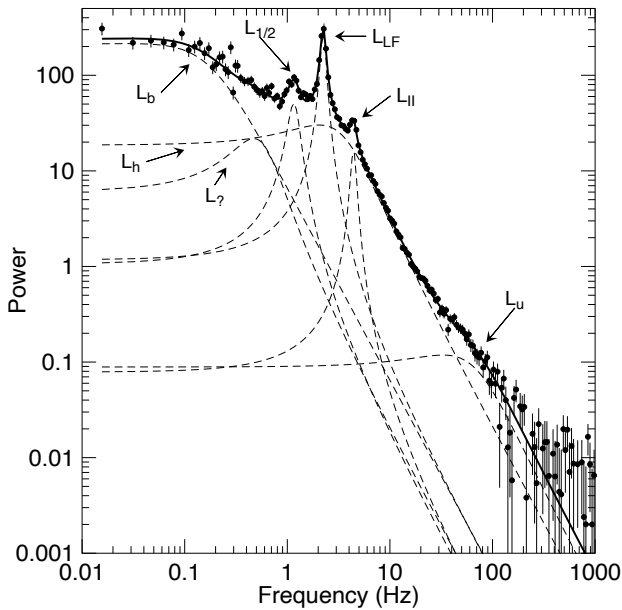


**Fig. 3.** Example of a PDS from GRS 1915+105 (RTXE observation 40703-01-01-00). The Lorentzian components fitted to the data are marked with dashed lines. The classifications of the peaks according to Belloni et al. (2002) is shown.

frequency, we classify also the other high-frequency peak at 143 Hz as a upper HFQPO.

Following the prescription in Ingram & Motta (2014) and by considering the BH mass for GRS 1915+105 from dynamical measurements, we are able to infer an additional, independent value of the spin to be compared with the value obtained above for consistency. We derive a second spin value,  $a_*^D = 0.71 \pm 0.13$ , which is consistent with the value we obtained above in Sec. 2.1.

### 3.2. Bringing in the PDS broad components

Finally, we consider the broad PDS components that have been associated with the HFQPOs in BH and NS X-ray binaries thanks to the well-known correlation discovered by Psaltis et al. (1999), the so-called Psaltis-Belloni-Van der Klis (PBK) correlation. While these broad-band components frequently appear in the PDS of BH X-ray binaries in general and in GRS 1915+105 in particular, their presence is not ubiquitous across all observations. Thus, instead of inspecting all the 1816 RXTE archival observations of GRS 1915+105, we focussed on the sample considered by Zhang et al. (2022), constructed based on the presence of broad-band signal at high frequencies (or a ‘‘bump’’).

Each observation was reduced following the standard procedures described in several works by our group (one recent example is Motta et al. 2022), with one main difference: since GRS 1915+105 is known for being a variable source, and changes in QPO centroid frequencies can happen on time-scales shorter than the average RXTE observation (a few thousands seconds spread across several satellite revolutions), we produced PDS employing 64 s long data segments and generated an average PDS accumulating a fixed number of segments (48) for a total of approximately 3000 s per average PDS, i.e. long enough to provide a good signal-to-noise-ratio in each spectrum, but not so long that the underlying power spectral density distribution varied significantly in the time interval considered, (thus violating the assumption of the Fourier analysis).

We generated a total of 480 average PDS using custom software under IDL (GHATS<sup>5</sup>), which we normalised according to Leahy et al. (1983) and we fitted with a combination of Lorentzian components. For all the PDS we calculated the characteristic frequency of all the Lorentzians components, defined as  $\nu_{\max} = \sqrt{\nu^2 + (\Delta/2)^2}$ , where  $\nu$  and  $\Delta$  are the frequency and width, respectively (see Belloni et al. 2002). Note that for narrow features such as QPOs the characteristic frequency is by construction very similar to the Lorentzian peak frequency.

While the PDS from GRS 1915+105 (and of BH binaries in general) can be complex, and it is often hard to classify components based on a given scheme (i.e., not all the components are all present all the time in every PDS), the majority of the components can be classified as follows, and as it is shown in Fig. 3. The PDS can include:

- a type-C QPO ( $L_{LF}$ ) and its harmonic content, i.e., a sub-harmonic ( $L_{1/2}$ ), a second harmonic ( $L_{II}$ ), and sometimes a third or fourth harmonic;
- a broad Lorentzian at low frequencies ( $L_b$ );
- a second broad Lorentzian peaking at frequency below the PDS break frequency ( $L_?$ );
- a third broad Lorentzian centred at a frequency close to the QPO centroid frequency ( $L_h$ );
- one or two broad Lorentzians at high frequencies ( $L_u$ ) and/or ( $L_l$ , not shown in the figure).

In the attempt to interpret the PDS components from GRS 1915+105 in an unbiased way, we plotted all the characteristic frequencies we found in all the PDS we generated in Fig. 2, together with the frequencies predicted by the RPM given the dynamical mass from photometry and the spin we calculated in Sec. 2.1. All frequencies increase with the frequency of the type-C QPO ( $L_{LF}$ ). In particular, in the context of the RPM, the Nodal Precession frequency corresponds to  $L_{LF}$ , and the sub-harmonic, second and third harmonic to this frequency correspond to  $L_{1/2}$ ,  $L_{II}$  and  $L_{III}$ . The periastron precession frequency and orbital frequency correspond to the broad components detected at high frequencies,  $L_l$  or  $L_u$ , respectively, or to HFQPOs (not shown in Fig. 3), as suggested by Psaltis et al. (1999).

In Fig. 3 several points do not clearly coincide with one of the frequencies of the RPM, and this is because the RPM aims to explain only three components of the several in the PDS. What is important to notice here is that several points are consistent with the frequencies predicted by the RPM for the mass and spins we derived from the 67 Hz QPOs under the assumption that they are the result of nodal precession of particles at ISCO. The vast majority of the points that are inconsistent with the RPM frequencies can be associated with the  $L_b$ ,  $L_h$  or  $L_?$  components (see Fig. 3).

### 3.3. Implications

The spin we obtained for the BH in GRS 1915+105 is the fourth one obtained via X-ray timing. Previous estimates were obtained for the BH X-ray binaries GRO J1655-40, XTE J1550-564, XTE J1859-226 presented in Motta et al. 2014a, Motta et al. 2014b, Motta et al. (2022), and the spins were 0.29, 0.34, and 0.15, respectively. In these cases, the spin values we derived are relatively low if compared to those typically obtained via other ‘electromagnetic’ spin measurement methods (continuum fitting, reflection

<sup>5</sup> [http://www.brera.inaf.it/utenti/belloni/GHATS\\_Package/Home.html](http://www.brera.inaf.it/utenti/belloni/GHATS_Package/Home.html)

**Table 1.** A summary of the quantities measured and derived in this work. Uncertainties are given at a 1-sigma level.

$M$	=	$12.4^{+2.0}_{-1.8} M_{\odot}$	Reid et al. (2014)
$a_*$	=	$0.706 \pm 0.034$	From 67Hz QPOs
$a_*^D$	=	$0.71 \pm 0.13$	From QPO doublet
$R_{\text{ISCO}}$	=	$3.36 \pm 0.15 R_g$	Derived
$\nu_{\text{nod@ISCO}}$	=	$67.712 \pm 2.056$ Hz	Measured
$\nu_{\text{HFQPO}}^{\text{upper}}$	=	$135.250 \pm 0.70$	Measured
$\nu_C$	=	$8.72 \pm 0.09$	Measured

spectroscopy, and reverberation, Reynolds 2021 for a recent review), which so far yielded spin distributions peaked at values above 0.9 (especially true in the case of the reflection-based measurements, see e.g. Draghis et al. 2023). Instead - and given the many peculiarities of this system this is perhaps unsurprising - the spin for GRS 1915+105 is relatively high - 0.76 - although still inconsistent with the value from X-ray spectroscopy (Miller et al. 2013).

While the number of timing-based spin values from the RPM is still low, they appear to be consistent with the BH spin distribution obtained based on the entire gravitational waves sample GWTC-3 (The LIGO Scientific Collaboration et al. 2021). This distribution peaks around spin  $\sim 0.2$  and shows a thin tail extending to higher values, thus indicating that the vast majority BHs in binary BH systems are relatively slow rotators. Unlike the case of other ‘electromagnetic’ methods, the results of which indicate that the spin distributions from binary BHs and BH X-ray binaries may be different (Draghis et al. 2023), our results seem to suggest that the LIGO/Virgo/KAGRA BHs and X-ray binary BHs may feature a similar spin distribution, and hence may be members of strictly related populations (see Belczynski et al. 2021; Fishbach & Kalogera 2022).

## 4. Conclusions

Building on the observation that the 67 Hz QPOs in GRS 1915+105 are confined to a narrow frequency range, we hypothesized these QPOs to be a consequence of nodal precession at the ISCO around a spinning black hole.

Using the Relativistic Precession Model and the black hole mass determined from dynamical measurements ( $M = 12.4^{+2.0}_{-1.8} M_{\odot}$ ), we derived a moderately high black hole spin ( $a^* = 0.706 \pm 0.034$ ). Our predictions of frequencies around a black hole with this spin and mass nicely matched the observational data, lending further support to the idea that certain PDS features in accreting BH X-ray binaries can be explained by matter motion near a compact object.

We conclude that the 67 Hz QPOs observed in GRS 1915+105, historically classified as HFQPOs, are more plausibly type-C QPOs originating from the vicinity of the ISCO of a moderately spinning black hole.

*Acknowledgements.* The authors acknowledge financial contribution from grant PRIN INAF 2019 n.15. This work benefited from discussions during Team Meetings of the International Space Science Institute (Bern), whose support we acknowledge.

SEM heartily thanks Tomaso Belloni, who sadly passed away before this paper could be completed. Among many other contributions to the field, his work was crucial for the understanding of GRS 1915+105.

SEM acknowledge the assistance of ChatGPT for proofreading and language enhancement in the preparation of this manuscript.

## References

- Altamirano, D., Belloni, T., Linares, M., et al. 2011, *ApJ*, 742, L17
- Belczynski, K., Done, C., & Lasota, J. P. 2021, arXiv e-prints, arXiv:2111.09401
- Belloni, T., Méndez, M., & Sánchez-Fernández, C. 2001, *A&A*, 372, 551
- Belloni, T., Psaltis, D., & van der Klis, M. 2002, *ApJ*, 572, 392
- Belloni, T. M. & Altamirano, D. 2013a, *MNRAS*, 432, 19
- Belloni, T. M. & Altamirano, D. 2013b, *MNRAS*, 432, 10
- Belloni, T. M., Bhattacharya, D., Caccese, P., et al. 2019, *MNRAS*, 489, 1037
- Belloni, T. M., Sanna, A., & Méndez, M. 2012, *MNRAS*, 426, 1701
- Belloni, T. M. & Stella, L. 2014, *Space Sci. Rev.*, 183, 43
- Casella, P., Belloni, T., Homan, J., & Stella, L. 2004, *A&A*, 426, 587
- Casella, P., Belloni, T., & Stella, L. 2005, *ApJ*, 629, 403
- Draghis, P. A., Miller, J. M., Zoghbi, A., et al. 2023, *ApJ*, 946, 19
- Fender, R. & Belloni, T. 2004, *ARA&A*, 42, 317
- Fishbach, M. & Kalogera, V. 2022, *ApJ*, 929, L26
- Fragile, P. C., Straub, O., & Blaes, O. 2016, *MNRAS*, 461, 1356
- Franchini, A., Motta, S. E., & Lodato, G. 2012, *MNRAS*, 467, 145
- Ingram, A., Done, C., & Fragile, P. C. 2009, *MNRAS*, 397, L101
- Ingram, A. & Motta, S. 2014, *MNRAS*, 444, 2065
- Ingram, A. R. & Motta, S. E. 2019, *New A Rev.*, 85, 101524
- Leahy, D. A., Elsner, R. F., & Weisskopf, M. C. 1983, *ApJ*, 272, 256
- Markwardt, C., Swank, J., Chen, X., & Taam, R. 1997, in *American Astronomical Society Meeting Abstracts*, Vol. 191, American Astronomical Society Meeting Abstracts, 111.03
- Miller, J. M., Parker, M. L., Fuerst, F., et al. 2013, *ArXiv e-prints* [arXiv:1308.4669]
- Morgan, E. H., Remillard, R. A., & Greiner, J. 1997, *ApJ*, 482, 993
- Motta, S., Belloni, T., & Homan, J. 2009, *MNRAS*, 400, 1603
- Motta, S. E., Belloni, T., Stella, L., et al. 2022, *MNRAS*, 517, 1469
- Motta, S. E., Belloni, T. M., Stella, L., Muñoz-Darias, T., & Fender, R. 2014a, *MNRAS*, 437, 2554
- Motta, S. E., Casella, P., Henze, M., et al. 2015, *MNRAS*, 447, 2059
- Motta, S. E. & Fender, R. P. 2019, *MNRAS*, 483, 3686
- Motta, S. E., Franchini, A., Lodato, G., & Mastroserio, G. 2018, *MNRAS*, 473, 431
- Motta, S. E., Kajava, J. J. E., Giustini, M., et al. 2021, *MNRAS*, 503, 152
- Motta, S. E., Muñoz-Darias, T., Sanna, A., et al. 2014b, *MNRAS*, 439, L65
- Motta, S. E., Rouco Escorial, A., Kuulkers, E., Muñoz-Darias, T., & Sanna, A. 2017, *MNRAS*, 468, 2311
- Psaltis, D., Belloni, T., & van der Klis, M. 1999, *ApJ*, 520, 262
- Ratti, E. M., Jonker, P. G., Miller-Jones, J. C. A., et al. 2012, *MNRAS*, 423, 2656
- Reid, M. J., McClintock, J. E., Steiner, J. F., et al. 2014, *ApJ*, 796, 2
- Remillard, R. A., Munro, M. P., McClintock, J. E., & Orosz, J. A. 2002, *ApJ*, 580, 1030
- Reynolds, C. S. 2021, *ARA&A*, 59 [arXiv:2011.08948]
- Soleri, P., Belloni, T., & Casella, P. 2008, *MNRAS*, 383, 1089
- Stella, L. & Vietri, M. 1998, *ApJ*, 492, L59+
- Stella, L. & Vietri, M. 1999, *Physical Review Letters*, 82, 17
- Stella, L., Vietri, M., & Morsink, S. M. 1999, *ApJ*, 524, L63
- Strohmayer, T. E. 2001, *ApJ*, 554, L169
- The LIGO Scientific Collaboration, the Virgo Collaboration, the KAGRA Collaboration, et al. 2021, arXiv e-prints, arXiv:2111.03606
- Vaughan, S. 2005, *A&A*, 431, 391
- Wijnands, R. & van der Klis, M. 1999, *ApJ*, 514, 939
- Zhang, Y., Méndez, M., García, F., et al. 2022, *MNRAS*, 514, 2891

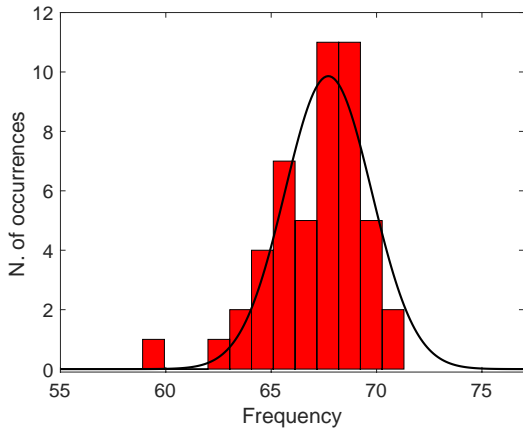


**Fig. A.1.** A Histograms of the centroid frequencies of the QPOs found around 67 Hz in the data from GRS 1915+105, as reported in Belloni & Altamirano (2013b). The black solid line is the best Gaussian fit to the histogram, which yields a centroid frequency of 67.712 Hz and a FWHM of 2.056 Hz.

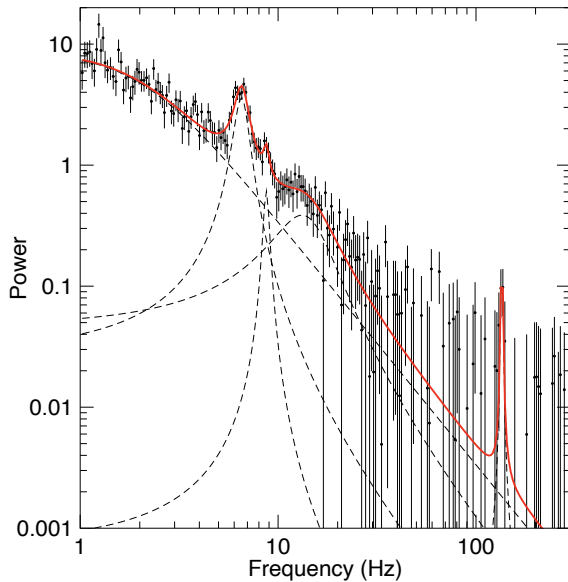


**Fig. A.2.** A PDS from observation 50703-01-10-02, which includes a type-B QPO at  $6.53 \pm 0.38$  Hz, a type-C QPO at  $8.71 \pm 0.09$  Hz, and a high frequency QPO at  $135.250 \pm 0.70$ .

### Appendix A: Additional figures

In this appendix we show additional figures to complement the analysis presented in the main text. In Fig. A.1 we show a histogram including the centroid frequencies of the 67 Hz QPOs reported in Belloni & Altamirano (2013b), save for the 2 peaks detected above 100 Hz.

Figure A.2 shows the PDS from observation 50703-01-10-02, including a type-B, a type-C, and a HFQPO. The broad peak at the high-frequency side of the LFQPOs is centered at  $\sim 13.2$  Hz, and could be the hint of a second harmonic to the type-B QPO (albeit significantly broader than what would be expected in this case), or a  $L_h$  component (see Fig. 3).

**Table A.1.** A summary of the quantities measured and derived in this work. Uncertainties are given at a 1-sigma level. The parameters marked by a † were fixed to the reported values. We note that the HFQPO has been reported in Belloni & Altamirano (2013b) as a significant feature after taking into account the number of trials.

Component	Centroid Frequency [Hz]	Width [Hz]	Leahy normalisation [counts/Hz]	rms [1-300 Hz] [1/Hz]
Broad component 1	0.0 <sup>†</sup>	4.0±0.3	30±1	0.84±0.03
Type-B QPO	6.53±0.05	1.2±0.1	6.4±0.5	0.19±0.01
Type-C QPO	8.7±0.1	0.6 <sup>†</sup>	0.6±0.2	0.018±0.006
Upper HFQPO	135.1 <sup>+0.6</sup> <sub>-0.8</sub>	1.73112 <sup>+3</sup> <sub>-1</sub>	0.7±0.2	0.20±0.006
Broad component 2	13.2 <sup>+0.7</sup> <sub>-0.8</sub>	10 <sup>+3</sup> <sub>-2</sub>	8.7 <sup>+0.9</sup> <sub>-0.8</sub>	0.157 <sup>+0.027</sup> <sub>-0.024</sub>
$\chi^2/\nu$		219.90/221		